Regge signatures from forward CLAS $\Lambda(1520)$ photoproduction data

En Wang,[1,*] Ju-Jun Xie,[2,3,4,†] and Juan Nieves[3,‡]

[1] *Departamento de Física Teórica and IFIC, Centro Mixto Universidad de Valencia-CSIC, Institutos de Investigación de Paterna, Aptd. 22085, E-46071 Valencia, Spain*

[2] *Institute of Modern Physics, Chinese Academy of Sciences, Lanzhou 730000, China*

[3] *Instituto de Física Corpuscular (IFIC), Centro Mixto CSIC-Universidad de Valencia, Institutos de Investigación de Paterna, Aptd. 22085, E-46071 Valencia, Spain*

[4] *State Key Laboratory of Theoretical Physics, Institute of Theoretical Physics, Chinese Academy of Sciences, Beijing 100190, China*

(Dated: May 14, 2014)

The $\gamma p \to K^+\Lambda(1520)$ reaction mechanism is investigated within a Regge–effective Lagrangian hybrid approach based on our previous study of this reaction [Physical Review C89, 015203 (2014)]. Near threshold and for large K^+ angles, both the CLAS and LEPS data can be successfully described by considering the contributions from the contact, t-channel $\bar{K}$ exchange, u-channel $\Lambda(1115)$ hyperon pole, and the s-channel nucleon pole and $N^*(2120)$ resonance contributions. However, for higher energies and forward K^+ angles, systematic discrepancies with data appear, which hint the possible existence of sizable quark-gluon string mechanism effects. We show how the inclusion of a $\bar{K}$ Regge–trajectory exchange in the t-channel leads to an efficient description of the $\Lambda(1520)$ photoproduction channel over the whole energy and angular ranges accessible in the CLAS experiment.

PACS numbers: 13.75.Cs.; 14.20.-c.; 13.60.Rj.

I. INTRODUCTION

The associate production of hadrons by photons has been extensively studied since it provides an excellent tool to learn details of the hadron spectrum. In particular, the $\gamma p \to K^+\Lambda(1520)$ reaction is an efficient isospin 1/2 filter for studying nucleon resonances decaying to $K\Lambda(1520)$. As a consequence, the experimental database on this reaction has expanded significantly in recent years. In addition to the pioneering measurements at Cornell [1], CEA [2], SLAC [3] and Daresbury [4] laboratories, in 2001 the CLAS Collaboration investigated this process in electroproduction [5] and later in 2010, this reaction has been examined at photon energies below 2.4 GeV in the SPring-8 LEPS experiment using a forward-angle spectrometer and polarized photons [6, 7], and from threshold to 2.65 GeV with the SAPHIR detector at the electron stretcher facility ELSA in Bonn [8]. Very recently, the exclusive $\Lambda(1520)$ photoproduction cross section has been measured by using the CLAS detector for energies from threshold up to an invariant γp mass $W = 2.85$ GeV [9].

In parallel to this great experimental activity, there have also been a large number of theoretical investigations of the $\Lambda(1520)$ ($\equiv \Lambda^*$) resonance production with the $\gamma p \to K^+\Lambda(1520)$ reaction. For invariant masses $W \leq 3$ GeV, most of these theoretical calculations [10–16] describe reasonably well the experimental data within the framework of effective Lagrangian approach. One of the latest of these works correspond to that of Ref. [15], where in addition to the contact, s-channel nucleon pole and t-channel $\bar{K}$ exchange contributions, which were already considered in previous works, the s-channel $N^*(2120)$ [previously called $N^*(2080)$] resonance and the u-channel $\Lambda(1115)$ hyperon pole terms were also included. The latter mechanism had been ignored in all previous calculations [10, 13, 14] that relied on the very forward K^+ angular LEPS data [6, 7], where its contribution was expected to be small. However, it produced an enhancement for large K^+ angles, and it become more and more relevant as the photon energy increases, being essential to describe the CLAS differential cross sections at backward angles. On the other hand, the combined analysis of the CLAS and LEPS data carried out in Ref. [15] provided further support on the existence of the $J^P = 3/2^-$ $N^*(2120)$ resonance, and additional constraints to its properties, confirming the previous findings of Refs. [13, 16]. Indeed, the model of Ref. [15] leads to an overall good description of both sets of data, both at forward and backward K^+ angles, and for the whole range of measured γp invariant masses in the CLAS and LEPS experiments. However, for invariant masses $W > 2.35$ GeV and forward angles, some small discrepancies (though systematic) between the CLAS data and the theoretical predictions appear (see lower panels of Fig. 3 of Ref. [15], collected here in the right panels of Fig. 1), which led to a moderate value of the best-fit $\chi^2/dof \sim 2.5$.

This should not be entirely surprising, since the model of Ref. [15] is not suited at high energies and forward angles, where quark-gluon string mechanisms could become important [17–19]. Actually, it is obvious from the analysis of the experimental hadron cross section data that the Reggeon and the Pomeron exchange mechanisms play a

*Electronic address: En.Wang@ific.uv.es

†Electronic address: xiejujun@impcas.ac.cn

‡Electronic address: jmnieves@ific.uv.es

crucial role at high energies and small transferred momenta [20, 21]. The underlying philosophy of the Regge formalism is as follows. In modeling the reaction amplitude for the $\gamma p \to KY$ process at high energies and small $|t|$ or $|u|$, instead of considering the exchange of a finite selection of individual particles, the exchange of entire Regge trajectories is taken into account. This exchange can take place in the t channel (kaonic trajectories) or u channel (hyperonic trajectories). As such, Regge theory offers an elegant way to circumvent the controversial issue of modeling high-spin, high-mass particle exchange.

Different dominant mechanisms have been proposed to describe the LAMP2 (Daresbury laboratory [4]) high energy differential cross sections. Thus, in Refs. [18, 19] it was claimed a large contribution from a t-channel $\bar{K}^*$ Regge exchange. However, in Ref. [17], it was argued that the $\bar{K}^*$ contribution should be quite small, almost negligible, since the $K^*N\Lambda^*$ coupling is expected to be much smaller than the value implicitly assumed in the previous works[1]. Nevertheless, a Reggeon exchange model, but with a $\bar{K}$- (instead of a $\bar{K}^*$) trajectory was also used in Ref. [17]. It was also discussed there that the $\bar{K}$ Reggeon mechanism is more favored by the LAMP2 data than the $\bar{K}^*$ Reggeon one, and that it is able to reproduce the available experimental data in the region from $E_\gamma^{\rm LAB} \sim 2.8$ GeV up to 5 GeV. Reggeized propagators for the $\bar{K}$ and $\bar{K}^*$ exchanges in the t-channel implemented in a gauge-invariant manner were employed in Ref. [23] and compared to Daresbury data. Note, however, that the $\bar{K}^*$ exchange contribution was also neglected in Ref. [23].

In this work, we aim to correlate the systematic (small) visible discrepancies, at high γp invariant masses and small angles, among the theoretical predictions of Ref. [15] and the CLAS data with Regge effects. To this end, we improve on the model of Ref. [15] by including the contribution of a $\bar{K}-$Regge trajectory exchange at high energies and low momentum transfers. We use a hybrid model which interpolates from the hadron effective Lagrangian approach, for energies close to threshold, to the quark-gluon string reaction mechanism approach, respecting gauge invariance.

Recently, it has appeared a work [24] with similar objectives and ideas. There, the crucial role played by the u-channel $\Lambda(1115)$ hyperon pole term at backward angles is confirmed, as well as the importance of the $N^*(2120)$ resonance to describe the LEPS data. Moreover, Regge effects are also discussed and taken into account, within a hybrid model that has indeed many formal resemblances[2] with the one that will be presented in this work. However, in sharp contrast with the model derived here, $\bar{K}^*$ Regge trajectory effects are considered in Ref. [24] and claimed to provide a considerable contribution at high energies. It is also claimed in this reference that the contribution from $\bar{K}$ and $\bar{K}^*$ exchange play a similar role in the reproduction of the CLAS data. Furthermore, the couplings of the $N^*(2120)$ state are fixed to those deduced in the constituent quark model of Refs. [25, 26], and a large width of 330 MeV is also set for this resonance. In this way, a great opportunity to take advantage of the accurate LEPS and CLAS data, not only for claiming the existence of the two-star $N^*(2120)$ state, but also for constraining/determining some of its poorly known properties is somehow missed in the analysis carried out in Ref. [24].

The present paper is organized as follows. In Sec. II, we shall discuss the formalism and the main ingredients of the model. In Sec. III, we will present our main results and finally, a short summary and conclusions will be given in Sec. IV.

II. FORMALISM AND INGREDIENTS

A. Feynman amplitudes

Within the effective Lagrangian approach for the $\Lambda(1520)$ photoproduction reaction,

$$\gamma(k_1,\lambda)p(k_2,s_p) \to K^+(p_1)\Lambda^*(p_2,s_{\Lambda^*}), \qquad (1)$$

the invariant scattering amplitudes are defined as

$$-iT_i = \bar{u}_\mu(p_2,s_{\Lambda^*})A_i^{\mu\nu}u(k_2,s_p)\epsilon_\nu(k_1,\lambda), \qquad (2)$$

where the kinematical variables (k_1,k_2,p_1,p_2) are defined as in Refs. [13, 15], with t, s and u, the Mandelstam variables: $t = q_t^2 = (k_1-p_1)^2$, $s = (k_1+k_2)^2$ and $u = q_u^2 = (p_2-k_1)^2$. On the other hand, u_μ and u are dimensionless Rarita-Schwinger and Dirac spinors, respectively, while $\epsilon_\nu(k_1,\lambda)$ is the photon polarization vector. In addition, s_p and s_{Λ^*} are the proton and $\Lambda(1520)$ polarization variables, respectively. The sub-index i stands for the contact, t-channel antikaon exchange, s-channel nucleon and $N^*(2120)$ ($\equiv N^*$) resonance pole terms (depicted in Fig. 1 of Ref. [13]) and the u-channel Λ pole mechanism (depicted in Fig. 2 of Ref. [15]). In Eq. (2), $A_i^{\mu\nu}$ are the reduced tree level amplitudes which can be obtained from the effective Lagrangian densities given in Refs. [13, 15]. For the sake of completeness, we also

[1] This is because the $\Lambda(1520)$ resonance is located very close to the threshold energy of the $\pi\Sigma^*$ channel, which dominates the $\Lambda(1520)$ dynamics. Indeed, it could be considered as bound state of these two hadrons, with some corrections from coupled channel dynamics. For very small binding energies, all the couplings of the resonance tend to zero as the mass of the bound state approaches the $\pi\Sigma^*$ threshold [22].

[2] Nevertheless, as we will explain below, some of the parameters found in Ref. [24] make difficult/doubtful the theoretical interpretation of the scheme of this reference, since t-channel Regge effects would have also been considered for large scattering angles.

present here these amplitudes (see Refs. [13, 15] for some more details):

$$A_t^{\mu\nu} = -e\frac{g_{KN\Lambda^*}}{m_K}\frac{1}{t-m_K^2}q_t^\mu(q_t^\nu - p_1^\nu)\gamma_5\, f_{\rm c}, \quad (3)$$

$$A_s^{\mu\nu} = -e\frac{g_{KN\Lambda^*}}{m_K}\frac{1}{s-m_N^2}\, p_1^\mu\gamma_5\,[\not k_1\gamma^\nu\, f_{\rm s} + (\not k_2 + m_N)\gamma^\nu\, f_{\rm c} + (\not k_1 + \not k_2 + m_N)i\,\frac{\kappa_p}{2m_N}\sigma_{\nu\rho}k_1^\rho\, f_{\rm s}\Big], \quad (4)$$

$$A_c^{\mu\nu} = e\frac{g_{KN\Lambda^*}}{m_K}g^{\mu\nu}\gamma_5\, f_{\rm c}, \quad (5)$$

$$A_R^{\mu\nu} = \gamma_5\left(\frac{g_1}{m_K}\not p_1 g^{\mu\rho} - \frac{g_2}{m_K^2}p_1^\mu p_1^\rho\right)\frac{\not k_1 + \not k_2 + M_{N^*}}{s - M_{N^*}^2 + iM_{N^*}\Gamma_{N^*}} \times P_{\rho\sigma}\left[\frac{ef_1}{2m_N}(k_1^\sigma\gamma^\nu - g^{\sigma\nu}\not k_1) + \frac{ef_2}{(2m_N)^2}(k_1^\sigma k_2^\nu - g^{\sigma\nu}k_1\cdot k_2)\right] f_R, \quad (6)$$

$$A_u^{\mu\nu} = \left[\frac{h_1}{2m_\Lambda}(k_1^\mu\gamma^\nu - g^{\mu\nu}\not k_1) + \frac{h_2}{(2m_\Lambda)^2}(k_1^\mu q_u^\nu - g^{\mu\nu}k_1\cdot q_u)\right] \times\frac{\not q_u + m_\Lambda}{u - m_\Lambda^2}g_{KN\Lambda}\gamma_5 f_u. \quad (7)$$

Form factors, needed because the hadrons are not point-like particles, have been also included in the above expressions. We use the following parametrization [27, 28]:

$$f_i = \frac{\Lambda_i^4}{\Lambda_i^4 + (q_i^2 - M_i^2)^2}, \quad i = s,\ t,\ R,\ u \quad (8)$$

$$f_c = f_s + f_t - f_s f_t, \quad \text{and} \begin{cases} q_s^2 = q_R^2 = s, \\ M_s = m_N, \\ M_t = m_K, \\ M_R = M_{N^*}, \\ M_u = m_\Lambda, \end{cases} \quad (9)$$

where the form of f_c is chosen such that the on-shell values of the coupling constants are reproduced and gauge invariance is preserved.

B. Regge contributions

We base our model on the exchange of a dominant $\bar{K}$ Regge trajectory in the t-channel, as suggested in Ref. [17]. The kaon trajectory represents the exchange of a family of particles with kaon-type internal quantum numbers. We will discuss two different models to include the Regge contribution in the present calculation [3]:

- model A: In this case, the kaon Regge trajectory contribution is obtained from the Feynman amplitude $A_t^{\mu\nu}$ of Eq. (3) by replacing the usual kaon pole-like Feynman propagator by a so-called Regge propagator, while keeping the rest of the vertex structure, i.e.,

$$\frac{1}{t-m_K^2} \to \left(\frac{s}{s_0}\right)^{\alpha_K}\frac{\pi\alpha'_K}{\Gamma(1+\alpha_K)\sin(\pi\alpha_K)}, \quad (10)$$

with $\alpha_K(t) = \alpha'_K(t-m_K^2) = 0.8\ \text{GeV}^{-2}\times(t-m_K^2)$, the linear Reggeon trajectory associated to the kaon quantum numbers. The constant s_0 is taken as the Mandelstam variable s at threshold [$s_0 = (m_K+M_{\Lambda^*})^2$], and it is introduced to fix the dimensions and to normalize the coupling constants. This approach is similar to that followed in Ref. [23], which was also adopted in Ref. [24]. The scattering amplitude for the Reggeon exchange will finally read

$$(A_t^{\mu\nu})^{\rm Regg} = -e\frac{\bar{g}_{KN\Lambda^*}}{t-m_K^2}q_t^\mu(q_t^\nu - p_1^\nu)\gamma_5\mathcal{F}_A^{\rm Regg}, \quad (11)$$

$$\mathcal{F}_A^{\rm Regg}(t) = \left(\frac{s}{s_0}\right)^{\alpha_K}\frac{\pi\alpha'_K(t-m_K^2)}{\Gamma(1+\alpha_K)\sin(\pi\alpha_K)}, \quad (12)$$

where $\bar{g}_{KN\Lambda^*} = g_{KN\Lambda^*}\times\hat{f}$, with $\hat{f}$ a overall normalization factor of the Reggeon exchange contribution. Actually, Reggeon couplings to mesons and baryons might be, in general, different by up to a factor of 2 [21]. This undetermined scale will be fitted to the available data.

Note that the Regge propagator of Eq. (10) has the property that it reduces to the Feynman propagator $1/(t-m_K^2)$ if one approaches the first pole on the trajectory (i.e. $t\to m_K^2$, and thus $\mathcal{F}_A^{\rm Regg}\to 1$). This means that the farther we go from the pole, the more the result of the Regge model will differ from conventional Feynman diagram based models.

- model B: In the region of negative t, the Reggeized propagator in Eq. (12) exhibits a factorial growth[4], which is in principle not acceptable [29]. Accordingly, the authors of Refs. [17, 21] proposed the use of a form factor that decreased with t and a simplified expression for the Regge contribution[5]

$$T_{\rm Regg} \sim \frac{e\bar{g}_{KN\Lambda^*}}{m_K}\left(\frac{s}{s_0}\right)^{\alpha_K(t)}F(t), \quad (13)$$

[3] We remind that when Reggeized propagators are employed the gauge invariance is broken, and that t-channel Regge effects should only be relevant for forward angles and high energies. These two points will be addressed below.

[4] Note, $[\Gamma(1+\alpha_K)\sin(\pi\alpha_K)]^{-1} = \Gamma(1-\alpha_K)/\pi\alpha_K$.

[5] In Refs. [17, 21], trajectories with a rotating ($e^{-i\pi\alpha_K(t)}$) phase, instead of a constant phase (see for instance the discussion in Ref. [30]) were assumed. The difference is an additional factor $(-1)^{\alpha_K(t)}$ in Eq. (13), which only affects to the interference between the Regge and hadronic contributions. Such interference occurs only in a limited window of γp invariant masses and t values, that is not well theoretically defined. Nevertheless, the CLAS data favor a constant phase as used in Eq. (13).

with $F(t)$ a Gaussian form factor that accounts for the compositeness of the external (incoming and outgoing) hadrons,

$$F(t) = e^{t/a^2}, \tag{14}$$

with a typical value of the cutoff parameter $a \sim 2$ GeV. By analogy with model A, we include in this context the Regge effects by replacing the form factor f_c in Eq. (3) by,

$$f_c \;\to\; \hat{f} \times \mathcal{F}_B^{\rm Regg} = \hat{f} \times \left(\frac{s}{s_0}\right)^{\alpha_K(t)} e^{t/a^2}\,. \tag{15}$$

1. Considerations on gauge invariance

The inclusion of Regge effects, in either of the two models discussed above, breaks gauge invariance. The amplitudes of the s-channel $N^*(2120)$ and the u-channel $\Lambda(1115)$ pole mechanisms are gauge invariant by themselves, while some cancelations among the t-channel $\bar{K}$ exchange, the s-channel nucleon pole and contact-term contributions are needed to fulfill gauge invariance. In the s-channel nucleon pole amplitude, the terms modulated by the form factor f_s are already gauge invariant. Thus, the cancelations mentioned refer only to the part of the T_s amplitude affected by the form factor f_c. We will denote this partial amplitude as T_s^*. Thus, any modification of the t-channel $\bar{K}$ exchange mechanism should have an appropriate counterpart in the nucleon pole and contact term contributions. To restore gauge invariance we follow the procedure discussed in Refs. [31, 32] and also adopted in [23], and replace $(T_t^{\rm Regg} + T_s^* + T_c)$ by

$$T_t^{\rm Regg} + (T_s^* + T_c) \times \hat{f} \times \mathcal{F}_{A,B}^{\rm Regg}\,. \tag{16}$$

2. Hybrid hadron and Reggeon exchange model

We propose a hybrid mechanism to study the $\gamma p \to K^+\Lambda(1520)$ reaction in the range of laboratory photon energies explored by the CLAS Collaboration data. At the lowest invariant masses, near threshold, we consider the effective Lagrangian model of Ref. [15], which amplitudes were collected in Subsec. II A. However, for the higher photon energies ($W > W_0$) and at low momentum transfers ($|t| < t_0$), or equivalently very forward K^+ angles, we assume that the string quark–gluon mechanism, discussed in Subsec. II B is dominant. Here, W_0 is a certain value of the γp invariant mass above which the Regge contribution starts becoming relevant. Similar considerations apply to the Mandelstam variable t, and its distinctive value t_0, which limits the kaon scattering angles where the Regge behaviour is visible. We will implement a smooth transition/interpolation between both reaction mechanisms [17], following the procedure adopted in Ref. [23]. Actually, we define/parametrize this hybrid model by using the invariant amplitudes of Eqs. (3)–(7), but replacing the form factor f_c by $\bar{f}_c$

$$f_c \to \bar{f}_c \;\equiv\; \mathcal{F}_{A,B}^{\rm Regg} \times \hat{f} \times \mathcal{R} + f_c(1-\mathcal{R}) \tag{17}$$

with

$$\mathcal{R} \;=\; \mathcal{R}_W \times \mathcal{R}_t, \tag{18}$$

$$\mathcal{R}_W \;=\; \frac{1}{1+e^{-(W-W_0)/\Delta W}}, \tag{19}$$

$$\mathcal{R}_t \;=\; \frac{1}{1+e^{(|t|-t_0)/\Delta t}}, \tag{20}$$

where we fix $W_0 = 2.35$ GeV and $\Delta W = 0.08$ GeV from the qualitative comparison of the predictions of Ref. [15] with the CLAS data and from the findings of Ref. [23]. In addition, we consider t_0 and Δt as free parameters that will be fitted to data.

It is easy to understand that $\mathcal{R}_W$ goes to one or to zero when $W \gg W_0$ or $W \ll W_0$, respectively, while $\mathcal{R}_t$ will tend to zero if $|t| \gg t_0$ and to one when $|t| \ll t_0$, as long as t_0 is sufficiently bigger than Δt. In this way, the amplitude of the reaction smoothly shifts from that determined from Eqs. (3)–(7) for $W \ll W_0$ to another one for $W \gg W_0$ that it is calculated using $T_t^{\rm Regg}$, instead of T_t, with the replacement of Eq. (16) implemented to preserve gauge invariance. Thus, Regge effects are incorporated with the variation of $\mathcal{R}_W$ from zero to one. Similar considerations apply to the variation of the Mandelstam variable t. The transition from the Regge model to the the effective Lagrangian one is controlled by the skin parameters ΔW and Δt.

Finally, we note that gauge invariance is accomplished at any value of $\mathcal{R}$.

C. Differential cross section

The unpolarized differential cross section in the center of mass (c.m.) frame for the $\gamma p \to K^+\Lambda(1520)$ reaction reads

$$\frac{d\sigma}{d\cos\theta_{\rm c.m.}} \;=\; \frac{m_N M_{\Lambda^*} |\vec{k}_1^{\,\rm c.m.}||\vec{p}_1^{\,\rm c.m.}|}{8\pi\,(s-m_N^2)^2} \sum_{\lambda, s_p, s_{\Lambda^*}} |T|^2, \tag{21}$$

where $\vec{k}_1^{\,\rm c.m.}$ and $\vec{p}_1^{\,\rm c.m.}$ are the photon and K^+ meson c.m. three-momenta, and $\theta_{\rm c.m.}$ is the K^+ polar scattering angle. The differential cross section $d\sigma/d(\cos\theta_{\rm c.m.})$ depends on W and also on $\cos\theta_{\rm c.m.}$.

In addition to the three new free parameters (t_0, Δt and $\hat{f}$) introduced to account for Regge effects, the model of Ref. [15] already had nine free parameters: i) the mass and width (M_{N^*} and Γ_{N^*}) of the $N^*(2120)$ resonance, ii) the cut off parameters $\Lambda_s = \Lambda_t = \Lambda_u \equiv \Lambda_B$ and Λ_R, and iii) the $N^*(2120)$ resonance electromagnetic $\gamma N N^*$ (ef_1, ef_2) and strong $N^*\Lambda^* K$ (g_1, g_2) couplings and the $\Lambda(1520)$ magnetic $\gamma\Lambda\Lambda^*$ (h_1) one. To reduce the number

of besfit parameters, we have kept unchanged the contribution of the u-channel Λ pole contribution, and thus we have set the $\gamma\Lambda\Lambda^*$ coupling to the value obtained in the Fit II of Ref. [15] ($h_1 = 0.64$). This is justified since the contribution of the u-channel Λ pole term is only important for backward K^+ angles, and the Regge mechanism should only play certain role at forward angles, In addition, we have also fixed Λ_B to the value of 620 MeV quoted in Ref. [15]. This cutoff parameter also appears in T_u, and in the definition of the form-factor f_c, which following Eq. (17) is replaced by $\bar{f}_c$ to account for Regge effects at high energies and low momentum transfers [6].

Thus, finally, we have ten free parameters which will be fitted to the recent differential cross section data from the CLAS [9] and LEPS [7] experiments.

III. NUMERICAL RESULTS AND DISCUSSION

We have performed a ten-parameter (g_1, g_2, Λ_R, ef_1, ef_2, M_{N^*}, Γ_{N^*}, t_0, Δt and $\hat{f}$) χ^2-fit to the LEPS [7] and CLAS [9] measurements of $d\sigma/d(\cos\theta_{\rm c.m.})$. There is a total of 216 available data (157 points from CLAS and another 59 ones from LEPS, depicted in Figs. 1 and 2, respectively). The systematical errors of the experimental data (11.6% [9] and 5.92% [7], for CLAS and LEPS, respectively) have been added in quadratures to the statistical ones and taken into account in the fits, as it was done in Ref. [15]. LEPS data lie in the K^+ forward angle region and were taken below $E_\gamma = 2.4$ GeV, while the recent CLAS measurements span a much larger K^+ angular and photon energy regions (nine intervals of the γp invariant mass from the reaction threshold, 2.02 GeV, up to 2.85 GeV) [7].

We have considered two different schemes to include Regge effects (models A and B), as discussed in Subsec. II B. Best fit results are listed in Table I, where we also compile the obtained parameters in our previous work (Fit II of Ref. [15]). For each fit, we also give the predicted $N^*(2120)$ partial decay width $\Gamma_{N^*\to\Lambda^* K}$ (Eq. (18) of Ref. [13]) and the resonance helicity amplitudes (Eqs. (15) and (16) of Ref. [13]) for the positive-charge state.

A χ^2/dof around 1.3 is obtained for both model A and B fits. This is significantly better than the best fit value obtained (2.5) in our previous work of Ref. [15], where Regge effects were not considered. We also see that the effective Lagrangian approach parameters (g_1, g_2, Λ_R, ef_1, ef_2, M_{N^*}, Γ_{N^*}), determined in the new fits carried out in this work, turn out to be in good agreement with those obtained in Ref. [15]. Thus, the conclusions of that reference still hold, in particular this new study gives further support to the existence of the two-star $N^*(2120)$ resonance, and its relevance in the CLAS & LEPS $\gamma p \to K^+\Lambda(1520)$ data. On the other hand, the hybrid model parameters (t_0, Δt and $\hat{f}$) turn out to be reasonable from what one would expect by a direct inspection of the CLAS data (t_0, Δt) and previous estimates [17, 21].

The fits obtained here are of similar quality to the best ones reported in Ref. [24], where in addition to the Regge effects driven by kaon exchange in the $t-$channel, some sizable Regge contributions induced by $\bar{K}^*$ exchanges are included as well. However, as mentioned in the introduction, theoretically it is difficult to accommodate a $\bar{K}^*$ mechanism contribution as large as that claimed in Ref. [24] (see sections 3.1 and 3.2 of this latter reference). On the other hand, a bunch of N^* resonances are included in the approach followed in Ref. [24]. Their couplings and masses are in most cases fixed to the constituent quark model predictions of Refs. [25, 26] and a common width of 330 MeV is assumed for all of them. Among all of them, it turns out to be the $N^*(2120)$, the state that provides the most important contribution, which confirms previous claims [13, 14] . We have adopted a different point of view and have used the accurate CLAS & LEPS $\gamma p \to K^+\Lambda(1520)$ data not only to claim the existence of the $N^*(2120)$ resonance, but also to establish some of its properties. Thus, we find a much narrower state ($\Gamma_{N^*} \sim 170-175$ MeV) and complete different helicity amplitudes. Moreover, the values used in Ref. [24] ($A^{p^*}_{1/2} = 36$ and $A^{p^*}_{3/2} = -43$ in $[10^{-3}\text{GeV}^{-1/2}]$ units) are incompatible both with

$$A^{p^*}_{1/2}[10^{-3}\text{GeV}^{-1/2}] \;=\; 125 \pm 45 \qquad (22)$$

$$A^{p^*}_{3/2}[10^{-2}\text{GeV}^{-1/2}] \;=\; 15 \pm 6\,, \qquad (23)$$

given in Ref. [33] and with previous measurements [34]

$$A^{p^*}_{1/2}[10^{-3}\text{GeV}^{-1/2}] \;=\; -20 \pm 8 \qquad (24)$$

$$A^{p^*}_{3/2}[10^{-2}\text{GeV}^{-1/2}] \;=\; 1.7 \pm 1.1 \qquad (25)$$

quoted in the 2008 PDG edition [35], that in turn are in quite good agreement with our predictions in Table I. Having improved the quality of our fit, achieving now an accurate description of the CLAS data for all angles and invariant mass windows (see below), our results give an important support to the measurements of Ref. [34], which do not seem entirely consistent with those reported in Ref. [33]. Given the two stars status (evidence of existence is only fair) granted to the $N^*(2120)$ resonance in the multichannel partial wave analysis of pion and photo-induced reactions off protons carried out in Ref. [33], the discrepancy with our predicted helicity amplitudes should not be used to rule out our fits, but rather one should interpret our results as further constrains on these

[6] Λ_B also appears in the definition of the f_s form-factor that affects to some pieces of the s-channel nucleon pole term. These contributions are however quite small since they are greatly suppressed by f_s, and do affect very little the best fit.

[7] To compute the cross sections in each interval, we always use the corresponding mean value of W, as in Ref. [15].

TABLE I: Values of some parameters determined in this work and in Ref. [15]. Model A(B) parameters have been adjusted to the combined LEPS [7] and CLAS [9] $\gamma p \to K^+\Lambda(1520)$ $d\sigma/d(\cos\theta_{\rm c.m.})$ data including Regge effects as discussed in Eq. (12) (Eq. (15)). In the last column, we compile some results from Fit II of Ref. [15], where the mechanism of Reggeon exchange was not considered. Finally, we also give for each fit, the predicted $N^*(2120)$ partial decay width $\Gamma_{N^*\to\Lambda^* K}$, and the helicity amplitudes for the positive-charge N^* state.

	This work		Ref. [15]
	model A	model B	Fit II
g_1	1.3 ± 0.2	1.4 ± 0.2	1.6 ± 0.2
g_2	0.9 ± 0.5	1.1 ± 0.5	2.2 ± 0.5
Λ_R [MeV]	1252 ± 78	1259 ± 76	1154 ± 47
ef_1	0.134 ± 0.016	0.123 ± 0.015	0.126 ± 0.012
ef_2	-0.110 ± 0.014	-0.100 ± 0.013	-0.097 ± 0.010
M_{N^*}[MeV]	2146 ± 5	2145 ± 5	2135 ± 4
Γ_{N^*}[MeV]	174 ± 14	171 ± 13	184 ± 11
t_0[GeV^2]	0.73 ± 0.04	0.94 ± 0.05	–
Δt[GeV^2]	0.28 ± 0.02	0.30 ± 0.04	–
$\hat{f}$	0.38 ± 0.01	0.37 ± 0.01	–
χ^2/dof	1.3	1.3	2.5
	Derived Observables		
$A^{p^*}_{1/2}[10^{-3}\text{GeV}^{-1/2}]$	-9.7 ± 4.1	-8.8 ± 3.8	-7.3 ± 3.0
$A^{p^*}_{3/2}[10^{-2}\text{GeV}^{-1/2}]$	2.3 ± 1.1	2.1 ± 1.0	2.5 ± 0.8
$\Gamma_{N^*\to\Lambda^* K}$ [MeV]	22 ± 7	25 ± 7	30 ± 8
$\frac{\Gamma_{N^*\to\Lambda^* K}}{\Gamma_{N^*}}$[%]	12.9 ± 3.9	14.8 ± 4.5	16.2 ± 4.2

elusive observables. Note that the helicity amplitudes given in Eqs. (24) and (25) were also used in Ref. [36], where the $ep \to eK^+\Lambda(1520)$ CLAS data of Ref. [5] was successfully described.

In addition, there is a disturbing feature in the fits presented in [24]. There, it is found $t_0 \sim 3$ GeV^2, though with a large error, while we obtain values in the range 0.7–0.9 GeV^2. A value of t_0 as high as 3 GeV^2 necessarily changes the meaning of the interpolating function $\mathcal{R}_t$ in Eq. (20), since it will not effectively filter now forward angles. This is easily understood if one realizes that for $W = 2.4$ GeV, $|t|$ remains below 2.5 GeV^2 for all possible K^+ c.m. angles, and for the highest invariant mass $W = 2.8$ GeV, the bound $t = -3$ GeV^2 is reached for $\cos\theta_{\rm c.m.} = -0.3$. Thus in the scheme employed in [24], the transition function $\mathcal{R}_t$ effectively modifies the predictions of the effective Lagrangian approach allowing for some Regge effects for large scattering angles, which seems quite doubtful. Probably, this dis-function of the physical meaning of $\mathcal{R}_t$ could be a consequence of the unnecessary complexity of the scheme used in Ref. [24] with various N^* contributions and the inclusion of $\bar{K}^*$ driven effects, with parameters in some cases fixed to values with little theoretical/experimental support. Nevertheless, it should be acknowledged that the work of Ref. [24] is pioneer in exploring the possible existence of Regge effects in the CLAS data.

The differential $d\sigma/d(\cos\theta_{\rm c.m.})$ distributions calculated with the model B best-fit parameters are shown in Figs. 1 and 2 as a function of $\cos\theta_{\rm c.m.}$ and for various γp invariant mass intervals. Model A results are totally similar and for brevity, they will not be discussed any further. Only statistical errors are displayed in these two figures and the contributions from different mechanisms are shown separately. Thus, we split the full result into three main contributions: effective Lagrangian approach background, Reggeon exchange and resonance $N^*(2120)$. The first one corresponds to the t-channel $\bar{K}$ exchange, nucleon pole, contact and u-channel $\Lambda(1115)$ hyperon pole terms of Eqs. (3)–(5) and (7), but evaluated with the modified form-factor $f_c(1-\mathcal{R})$ instead of f_c, as discussed in Eq. (17). (Note that f_c appears neither in the $\Lambda(1115)$ nor in the resonance $N^*(2120)$ mechanisms because both of them are gauge invariant by themselves). The Reggeon contribution is calculated from the f_c terms of the $\bar{K}$ exchange, nucleon pole and contact terms of Eqs. (3)–(5) and (7), but now evaluated with the generalized Regge form-factor $\mathcal{F}_B^{\rm Regg}\hat{f}\mathcal{R}$.

In the left panels of the first of these two figures, we show our predictions and the data of the CLAS collaboration [9]. In the right panels and for comparison purposes, we display the final results from our previous Fit II carried out in Ref. [15], where Regge effects were not considered. We find an overall good description of the data for the whole range of measured γp invariant masses and it is significantly better than that exhibited in the right panels. We see that the Regge improved model provides now an excellent description of the CLAS data for val-

ues of $\cos\theta_{\rm c.m.}$ above 0.5, and high energies, $W \geq 2.3$ GeV, as expected. On the other hand, by construction Regge contributions effectively disappear at low invariant masses $W < 2.3$ GeV and backward K^+ angles. Thus, we recover for this latter kinematics the effective Lagrangian approach, including resonance $N^*(2120)$ and hyperon $\Lambda(1115)$ contributions, which successfully described the data in this region [15].

In the left panels of Fig. 2, the differential cross section deduced from the results of the model B fit, as a function of the LAB frame photon energy and for different forward c.m. K^+ angles, is shown and compared both to LEPS [7] and CLAS [9] datasets. In the right panels and for the sake of clarity, we display the final results from our previous Fit II carried out in Ref. [15], where Regge effects were not considered. We see the description of LEPS data is almost not affected by the Regge contributions, and the bump structure in the differential cross section at forward K^+ angles is fairly well described thanks to the significant contribution from the N^* resonance in the $s-$channel, as pointed out in Ref. [13, 15]. However, the inclusion of Regge effects significantly improves the description of the CLAS data [8], as one would expect from the discussion of the results of Fig. 1. Moreover, the hybrid model presented in this work provides a better energy behavior for the forward cross section at energies higher than those explored by the CLAS data (see the two (d) panels in Fig. 2).

Fig. 3 shows the $\Lambda(1520)$ total photoproduction cross section as a function of the photon energy. Despite the overall normalization of the CLAS [9] measurements [9] is in rather strong disagreement with the data from LAMP2 [4], the photon energy dependence of both data sets seems compatible above 2.3 or 2.4 GeV. This can be appreciated in Fig. 3, where the LAMP2 cross sections have been scaled down by a factor 0.6. This agreement might give some support to the idea of finding Regge signatures in the CLAS data. Results from model B are also shown, which turn out to provide a good description of both sets of data. We should, however, prevent the reader about the *ad hoc* modification of the normalization of the old LAMP2 cross sections [10]. Nevertheless, it is reassuring that the hybrid model presented in this work, including Regge effects, is able to predict the photon energy dependence of the LAMP2 data at energies well above than those explored by the CLAS data.

[8] The CLAS cross sections shown in the figure were obtained from the appropriate CLAS measurements displayed in Fig. 1, relating W to the LAB photon energy.

[9] We display extrapolated total cross sections, from data summed over the useful acceptance of the detector, to 4π (red points in Fig. 11 of Ref. [9]).

[10] The low energy SAPHIR data [8] is in even in a stronger disagreement with the data from LAMP2, with the CLAS results lying almost exactly between these two measurements [9].

IV. CONCLUSIONS

We have presented some evidences of Regge signatures in the CLAS data at forward angles, despite the energies involved in that experiment are only moderately high. This is not entirely surprising, because above $E_\gamma > 2.3 - 2.4$ GeV, and up to an overall normalization, the CLAS $\Lambda(1520)$ total cross section dependence on the photon energy matches that inferred from the LAMP2 data, which extends up to 5 GeV, in a region where the Regge behavior is expected to be visible (see Fig. 3). Indeed, we find a significant improvement on the description of the CLAS high energy forward cross sections, when the effective Lagrangian approach of Ref. [15] is supplemented with some string quark–gluon mechanism contributions determined by a kaon trajectory. Now, there are no visible systematic discrepancies between the hybrid approach predictions and the data. Thus, we confirm the findings of the recent work of Ref. [24] on the importance of the Regge effects in achieving an accurate description of the CLAS forward angular distributions.

We do not need to include any contribution from a $\bar{K}^*$ trajectory, in accordance to the analysis of the LAMP2 data carried out in Refs. [17, 23]. This is re-assuring since the $t-$channel $\bar{K}^*$ contribution should be quite small, almost negligible, in sharp contrast with previous works [10, 18, 19, 24], where a large $g_{K^*N\Lambda^*}$ coupling was assumed. Such big values for this coupling are ruled out by unitarized chiral models [17, 37, 38], that predict values for $g_{K^*N\Lambda^*}$ around a factor 10 (20) smaller than for instance those used in Refs. [10, 18, 24], and by measurements of the photon-beam asymmetry, as discussed in Ref. [23].

We have designed a gauge invariant hybrid model which smoothly interpolates from the hadron effective Lagrangian approach [15], at energies close to threshold, to a model that incorporates quark-gluon string reaction mechanism contributions at high energies and forward K^+ scattering angles. We find an accurate description of both CLAS and LEPS data. The latter set of low energy cross sections is not affected by the inclusion of Regge effects. The bump structure observed at forward K^+ angles in these data is well described thanks to the significant contribution from the two-star $J^P = 3/2^-$ $N^*(2120)$ resonance in the s-channel, which existence gets a strong support from this improved analysis that is now fully consistent with the accurate CLAS data. Thus, this associated strangeness production reaction becomes an excellent tool to determine the properties of this resonance (helicity amplitudes determined by the couplings ef_1 and ef_2 or the strength of the $K\Lambda^*N^*$ vertex). In what respects to the CLAS data, Regge effects play a crucial role at forward angles for energies above 2.35 GeV, as commented before, while the backward angle data highlight the importance of the u-channel $\Lambda(1115)$ hyperon pole term. This latter fact can be used to constrain the radiative $\Lambda^* \to \Lambda\gamma$ decay, as it was firstly emphasized in Ref. [15].

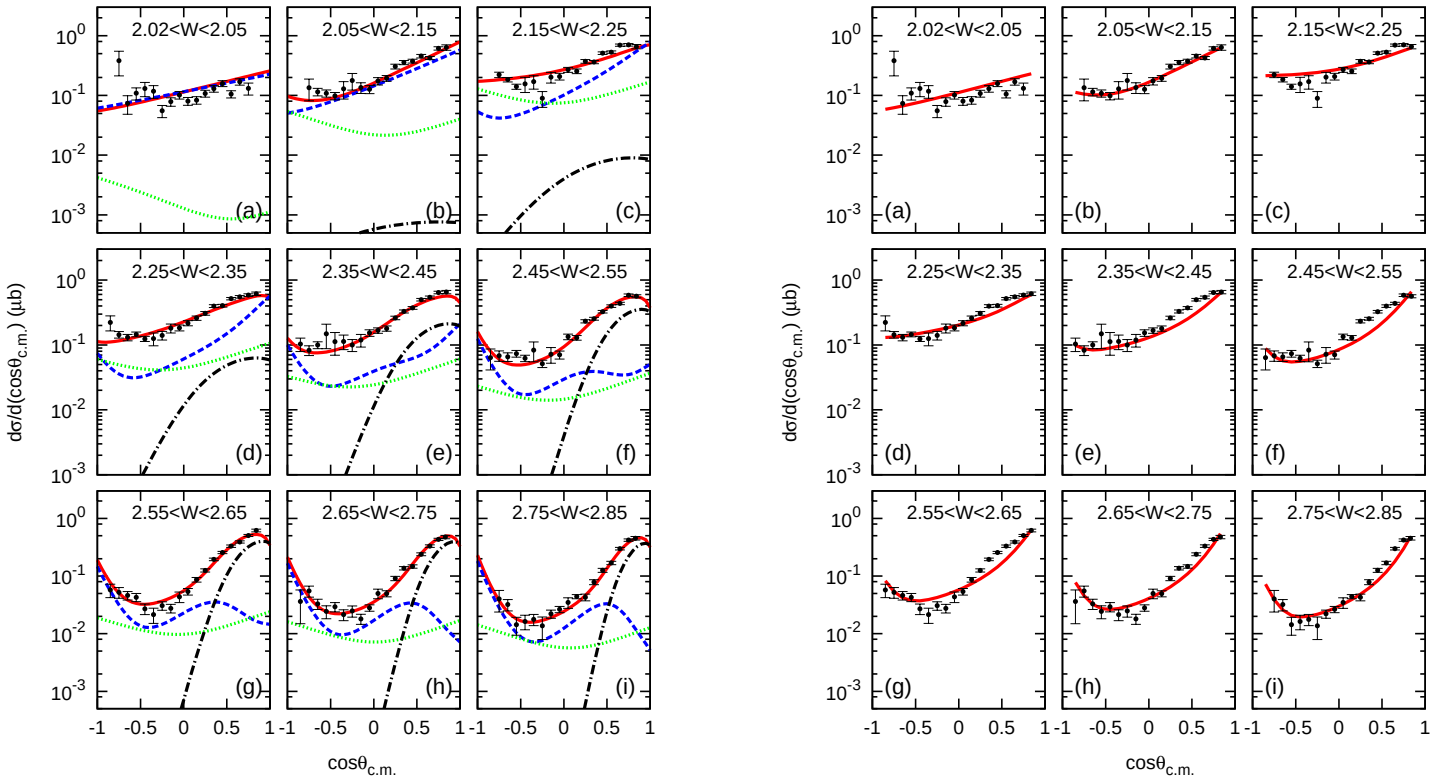

FIG. 1: (Color online) Left: Model B $\gamma p \to K^+\Lambda(1520)$ differential cross sections as a function of $\cos\theta_{\rm c.m.}$ compared with the CLAS data [9] for different γp invariant mass intervals (indicated in the different panels in GeV units). Only statistical errors are displayed. The blue-dashed and black-dash-dotted curves stand for the contributions from the effective Lagrangian approach background and Reggeon exchange mechanism, respectively (see text for details). The green-dotted lines show the contribution of the $N^*(2120)$ resonance term, while the red-solid lines display the results obtained from the full model. Right: Total results from our previous Fit II carried out in Ref. [15]), where Regge effects were not considered.

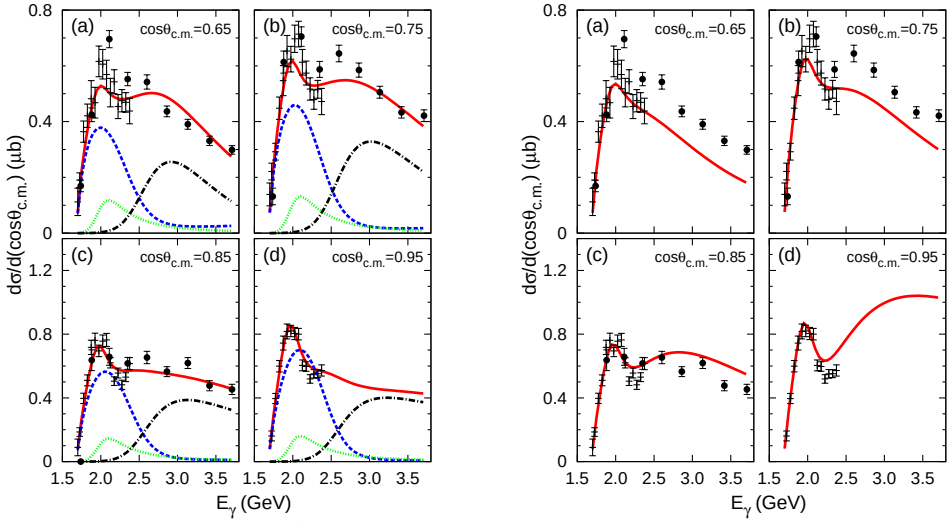

FIG. 2: (Color online) Left: Model B $\gamma p \to K^+\Lambda(1520)$ differential cross section as a function of the LAB frame photon energy for different c.m. K^+ polar angles. We also show the experimental LEPS [7] (crosses) and CLAS [9] (black dots) data. Only statistical errors are displayed. The blue-dashed and black-dash-dotted curves stand for the contributions from the effective Lagrangian approach background and Reggeon exchange mechanism, respectively (see text for details). The green-dotted lines show the contribution of the $N^*(2120)$ resonance term, while the red-solid lines display the results obtained from the full model. Right: Total results from our previous Fit II carried out in Ref. [15]), where Regge effects were not considered.

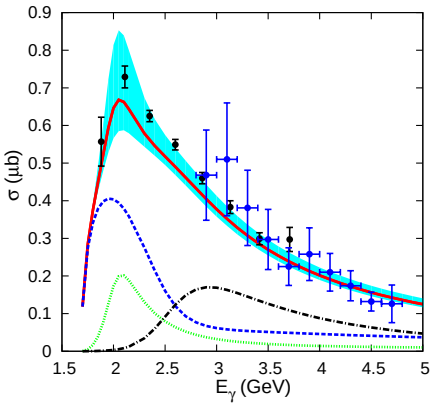

FIG. 3: (Color online) Total $\gamma p \to K^+\Lambda^*$ cross section as a function of the photon energy. Black filled circles and blue open circles stand for CLAS [9] and LAMP2 [4] data, respectively. LAMP2 cross sections have been scaled down by a factor 0.6. Results from model B are also shown: The blue-dashed and black-dash-dotted curves stand for the contributions from the effective Lagrangian approach background and Reggeon exchange mechanism, respectively (see text for details). The green-dotted lines show the contribution of the $N^*(2120)$ resonance term, while the red-solid lines display the results obtained from the full model. The shaded region accounts for the 68% CL band inherited from the Gaussian correlated statistical errors of the parameters.

The t-range explored by the CLAS data is not large enough to fully restrict the Regge form-factor, which is the major difference among the two models (A and B) introduced in this work. Though, in the region of negative t, the Reggeized propagator in Eq. (12) exhibits a factorial growth, which is in principle not acceptable, the limited range of momentum transfers accessible in the data does not see this unwanted behaviour. This is the same reason why the Gaussian cutoff parameter a in Eq. (14) is not further constrained. Unfortunately, the existing large discrepancies among CLAS and LAMP2 data sets prevents the inclusion of this latter experiment in the analysis carried out in this work. This constitutes an open problem, that might require new dedicated experiments.

Acknowledgments

This work was partly supported by DGI and FEDER funds, under Contract No. FIS2011-28853-C02-01 and FIS2011-28853-C02-02, the Spanish Ingenio-Consolider 2010 Program CPAN (CSD2007-00042), Generalitat Valenciana under Contract No. PROMETEO/2009/0090, and by the National Natural Science Foundation of China under Grant No. 11105126. We acknowledge the support of the European Community-Research Infrastructure Integrating Activity Study of Strongly Interacting Matter (HadronPhysics3; Grant Agreement No. 283286) under the Seventh Framework Programme of the E.U. The work was supported in part by DFG (SFB/TR 16, Subnuclear Structure of Matter.

[1] N. Mistry, S. Mori, D. Sober, and A. Sadoff, Phys. Lett. B **24**, 528 (1967).
[2] W. Blanpied, J. Greenberg, V. Hughes, P. Kitching, and D. Lu, Phys. Rev. Lett. **14**, 741 (1965).
[3] A. M. Boyarski et al., Phys. Lett. B **34**, 547 (1971).
[4] D. P. Barber, J. B. Dainton, L. C. Y. Lee, R. Marshall, J. C. Thompson, D. T. Williams, T. J. Brodbeck and G. Frost *et al.*, Z. Phys. C **7**, 17 (1980).
[5] S. P. Barrow *et al.* [CLAS Collaboration], Phys. Rev. C **64**, 044601 (2001).
[6] N. Muramatsu et al. (LEPS Collaboration), Phys. Rev. Lett. **103**, 012001 (2009).
[7] H. Kohri et al. (LEPS Collaboration), Phys. Rev. Lett. **104**, 172001 (2010).
[8] F. W. Wieland, J. Barth, K. H. Glander, J. Hannappel, N. Jopen, F. Klein, E. Klempt and R. Lawall *et al.*, Eur. Phys. J. A **47**, 47 (2011) [Erratum-ibid. A **47**, 133 (2011)].
[9] K. Moriya *et al.* [CLAS Collaboration], Phys. Rev. C **88**, 045201 (2013).
[10] S. -I. Nam, A. Hosaka and H. -C. Kim, Phys. Rev. D **71**, 114012 (2005).
[11] S. -I. Nam, K. -S. Choi, A. Hosaka and H. -C. Kim, Phys. Rev. D **75**, 014027 (2007).
[12] S. -I. Nam, Phys. Rev. C **81**, 015201 (2010).
[13] J. -J. Xie and J. Nieves, Phys. Rev. C **82**, 045205 (2010).
[14] J. He and X. -R. Chen, Phys. Rev. C **86**, 035204 (2012).
[15] J. -J. Xie, E. Wang and J. Nieves, Phys. Rev. C **89**, 015203 (2014).
[16] S. -I. Nam, J. Phys. G **40**, 115001 (2013).
[17] H. Toki, C. García-Recio, and J. Nieves, Phys. Rev. D **77**, 034001 (2008).
[18] A. I. Titov, B. Kämpfer, S. Daté, and Y. Ohashi, Phys. Rev. C **72**, 035206 (2005); ibid **C 74**, 055206 (2006).
[19] A. Sibirtsev, J. Haidenbauer, S. Krewald, U.-G. Meißner, and A. W. Thomas, Eur. Phys. J. A **31**, 221 (2007).
[20] A. Donnachie and P. V. Landshoff, Phys. Lett. B **185**, 403 (1987).
[21] V. Y. Grishina, L. A. Kondratyuk, W. Cassing, M. Mirazita and P. Rossi, Eur. Phys. J. A **25**, 141 (2005).
[22] S. Weinberg, Phys. Rev. **137**, B672 (1965).
[23] S. -I. Nam and C. -W. Kao, Phys. Rev. C **81**, 055206 (2010).
[24] J. He, Nucl. Phys. A **927**, 24 (2014).
[25] S. Capstick, Phys. Rev. D **46**, 2864 (1992).
[26] S. Capstick, and W. Roberts, Phys. Rev. D **58**, 074011 (1998).
[27] H. Haberzettl, C. Bennhold, T. Mart and T. Feuster, Phys. Rev. C **58**, 40 (1998).
[28] R. M. Davidson and R. Workman, Phys. Rev. C **63**, 025210 (2001).
[29] W. Cassing, L. A. Kondratyuk, G. I. Lykasov and

M. V. Rzjanin, Phys. Lett. B **513**, 1 (2001).
[30] M. Guidal, J. M. Laget and M. Vanderhaeghen, Nucl. Phys. A **627**, 645 (1997).
[31] T. Corthals, J. Ryckebusch and T. Van Cauteren, Phys. Rev. C **73**, 045207 (2006).
[32] T. Corthals, T. Van Cauteren, J. Ryckebusch, and D. G. Ireland, Phys. Rev. C **75**, 045204 (2007).
[33] A. V. Anisovich, R. Beck, E. Klempt, V. A. Nikonov, A. V. Sarantsev and U. Thoma, Eur. Phys. J. A **48**, 15 (2012).
[34] R. Kajikawa, eConf C **810824**, 352 (1981).
[35] C. Amsler *et al.* [Particle Data Group Collaboration], Phys. Lett. B **667**, 1 (2008).
[36] S. I. Nam, J. Phys. G **40**, 115001 (2013).
[37] T. Hyodo, S. Sarkar, A. Hosaka and E. Oset, Phys. Rev. C **73**, 035209 (2006) [Erratum-ibid. C **75**, 029901 (2007)].
[38] D. Gamermann, C. Garcia-Recio, J. Nieves and L. L. Salcedo, Phys. Rev. D **84**, 056017 (2011).